Pergamon

Bulletin of Mathematical Biology, Vol. 57, No. 6, pp. 809–840, 1995
Elsevier Science Inc.

0092–8240/95 $9.50 + 0.00

0092–8240(95)00026–M

DYNAMICS AND BIFURCATIONS OF TWO COUPLED NEURAL OSCILLATORS WITH DIFFERENT CONNECTION TYPES

■ GALINA N. BORISYUK,* ROMAN M. BORISYUK,* ALEXANDER I. KHIBNIK*† and DIRK ROOSE‡
*Institute of Mathematical Problems in Biology,
Russian Academy of Sciences,
Pushchino, Moscow Region,
142292 Russia

(*E.mail: borisyuk@impb.serpukhov.su*)

†Theory Center,
Cornell University,
Ithaca,
NY 14853, U.S.A.

(*E.mail: khibnik@cam.cornell.edu*)

‡Department of Computer Science,
Katholieke Universiteit Leuven,
B-3001 Leuven,
Belgium

(*E.mail: Dirk.Roose@cs.kuleuven.ac.be*)

In this paper we present an oscillatory neural network composed of two coupled neural oscillators of the Wilson–Cowan type. Each of the oscillators describes the dynamics of average activities of excitatory and inhibitory populations of neurons. The network serves as a model for several possible network architectures. We study how the type and the strength of the connections between the oscillators affect the dynamics of the neural network. We investigate, separately from each other, four possible connection types (excitatory→excitatory, excitatory→inhibitory, inhibitory→excitatory, and inhibitory→inhibitory) and compute the corresponding bifurcation diagrams. In case of weak connections (small strength), the connection of populations of different types lead to periodic *in-phase* oscillations, while the connection of populations of the same type lead to periodic *anti-phase* oscillations. For intermediate connection strengths, the networks can enter quasiperiodic or chaotic regimes, and can also exhibit multistability. More generally, our analysis highlights the great diversity of the response of neural networks to a change of the connection strength, for different connection architectures. In the discussion, we address in particular the problem of information coding in the brain using quasiperiodic and chaotic oscillations. In modeling low levels of information processing, we

propose that feature binding should be sought as a temporally coherent phase-locking of neural activity. This phase-locking is provided by one or more interacting convergent zones and does not require a central "top level" subcortical circuit (e.g. the septo-hippocampal system). We build a two layer model to show that although the application of a complex stimulus usually leads to different convergent zones with high frequency oscillations, it is nevertheless possible to synchronize these oscillations at a lower frequency level using envelope oscillations. This is interpreted as a feature binding of a complex stimulus.

1. Introduction. Recent neurophysiological experiments provide evidence that the primary processing of sensory stimuli can be connected to the appearance of oscillatory activity, both at the level of individual neurons and at the level of populations of neurons. Oscillations have been detected in experiments on the olfactory bulb (Freeman, 1991) and in primary areas of visual cortex (Eckhorn *et al.*, 1988; Gray and Singer, 1989; Gray *et al.*, 1989). Such periodic behavior suggests that synchronization of oscillations plays an essential role in neural information processing (see the discussion in Gray *et al.*, 1990). Investigations of motor activity demonstrate that certain patterns of oscillations correspond to different types of movements (Kelso *et al.*, 1986). Experimental data on the theta-rhythmic activity in the septo-hippocampal region correlate with memory and attention (Miller, 1991; Vinogradova *et al.*, 1991).

These experimental results have stimulated the development of mathematical models of oscillatory neural networks in which oscillations are the major feature (Borisyuk *et al.*, 1992a). For example, oscillatory neural networks may be used to model

- stimuli recognition in the olfactory system (Baird, 1986; Freeman *et al.*, 1988; Li and Hopfield, 1989; Wilson and Bower, 1988);
- response to simple visual stimuli in visual cortex (Borisyuk *et al.*, 1990; Eckhorn *et al.*, 1988; Fincel and Edelman, 1989; Sporns *et al.*, 1991; König and Shillen, 1991; Shillen and König, 1991; Shuster and Wagner, 1990a,b; Sompolinsky *et al.*, 1990a,b, 1991);
- control of locomotion (Kelso *et al.*, 1986; Kopell, 1988; Schöner *et al.*, 1990);
- data memorization (Abbott, 1990; Kazanovich *et al.*, 1991; Wang *et al.*, 1990); and
- integration of stimulus features in a total image and realization of the attention function (Borisyuk, 1991; Kryukov, 1991; von der Malsburg and Schneider, 1986).

In this paper we present an oscillatory neural network composed of two coupled identical neural ocillators with a symmetric coupling. This network serves as a model for several possible architectures and can be used to study how the connection type and the connection strength affect the dynamics of a neural network. We analyse the dynamical behavior of the system for

connection strengths varying over a large range of parameters. Our tools come from bifurcation analysis of dynamical systems.

There are many papers devoted to the investigation of the dynamical behavior of two coupled neural oscillators (e.g. Aronson *et al.*, 1990; Ermentrout and Kopell, 1991, etc.). Some neural oscillator models consider oscillations as an endogenous property of a pacemaker neuron:

- Van der Pol model (Kawato *et al.*, 1979);
- Hindmarsh–Rose model (1982); and
- Hodgkin–Huxley model (Hansel *et al.*, 1993); etc.

Another approach suggests that oscillations arise as a result of the interactions between neural populations, for example, between excitatory and inhibitory populations:

- Wilson–Cowan model (Wilson and Cowan, 1972; Borisyuk *et al.*, 1992b);
- "integrate and fire" model (Kryukov *et al.*, 1990; Borisyuk *et al.*, 1990); and
- McGregor model (1987), etc.

For most of these models, weak connections were emphasized and analysed using perturbation and phase reduction methods. The synchronization of two identical oscillators was studied and the following oscillatory modes, under different parameter values, were observed:

- in-phase oscillations (zero phase shift);
- anti-phase oscillations (half-period phase shift);
- out-of-phase oscillations (stationary phase shift which is different from zero and half-period); and
- multistability, for example, both in-phase and anti-phase oscillations.

In particular, it was shown by computer simulation (Kawato *et al.*, 1979) that for two Van der Pol oscillators with electrical coupling, both in-phase and anti-phase oscillations exist for the same parameter values. Hansel *et al.* (1993) considered the Hodgkin–Huxley neuron model with weak excitatory interaction using a phase reduction technique. He found out-of-phase oscillations with reduced firing rate in comparison with a single neuron. Wang and Rinzel (1992) obtained for inhibitory connections of two Hodgkin–Huxley neurons both anti-phase oscillations for instantaneous coupling and in-phase oscillations for a slowly decaying postsynaptic current. Cymbalyuk *et al.* (1994) showed that for the Hindmarsh–Rose neuron model with weak electrical coupling, all oscillatory modes mentioned above are possible under variation of the external current.

The main functional unit of oscillatory neural networks is a neural oscillator. In the present paper, we use the Wilson–Cowan model for a neural oscillator (Wilson and Cowan, 1972), that describes the dynamics of average activities of two neural populations, one excitatory and the other inhibitory. This model is based on mean field theory and allows a drastic reduction in the number of

variables in large scale models of neural activity. The dynamic behavior of average activity of the populations of the neural model can be compared with local field potentials and EEG's recorded with a macroelectrode. The Wilson–Cowan neural oscillator or similar models are used by many authors, for example, Freeman (1987), Yao and Freeman (1990)—to simulate chaotic EEG patterns of the olfactory system; Shuster and Wagner (1990), Borisyuk *et al.* (1990), Schillen and Konig (1991)—to simulate stimulus dependent oscillatory response of visual cortex; Shinomoto (1987), Wang *et al.* (1990)—to model associative memory.

Having chosen a simple architecture of the network in the form of two coupled oscillators, the design of the detailed structure of the (inter) connections between neuronal populations of both oscillators is still required. Our goal is to analyse each possible connection type individually.

To discuss the phenomena occurring in the network when the connection strength varies, we use ideas and terminology from bifurcation theory of dynamical systems. The bulk of our analysis is based on numerical simulations: we use the interactive software package LOCBIF (Khibnik *et al.*, 1993a,b) to detect and to analyse bifurcations of equilibria and limit cycles numerically, and we use the program TraX (Levitin, 1989; Khibnik, 1990) to explore dynamics, including Poincaré mappings and quasiperiodic motions.

The outline of the paper is as follows. In section 2 we introduce the model and we describe the connections we use to construct the network. In section 3 we present the classification of periodic solutions and discuss the case of weak connections. Sections 4–7 are devoted to the examination of bifurcation diagrams for each connection type. Section 8 contains conclusions and discusses the significance of chaotic and quasiperiodic regimes for neural information processing.

2. Model.

2.1. *A single-oscillator model.* We consider the Wilson–Cowan model (Wilson and Cowan, 1972) as a single neural oscillator. This model is represented by a system of two autonomous differential equations describing the dynamics of average activities of the excitatory and the inhibitory populations (measured as a portion of firing neurons in each population). Denoting these activities by E and I, respectively, the model reads:

$$\begin{aligned} \mathrm{d}E/\mathrm{d}t &= -E+(k_e-E)\cdot S_e(c_1E-c_2I+P) \\ \mathrm{d}I/\mathrm{d}t &= -I+(k_i-I)\cdot S_i(c_3E-c_4I+Q)\,. \end{aligned} \tag{1}$$

Here $S_e(x)=S(x, b_e, \theta_e)$ and $S_i(x)=S(x, b_i, \theta_i)$ are monotonically increasing sigmoid-type functions given by the formula

$$S(x, b, \theta) = 1/(1+\exp(-b(x-\theta))) - 1/(1+\exp(b\theta)),$$

k_e and k_i are constants, $k_e = S_e(+\infty)$, $k_i = S_i(+\infty)$, P and Q are the external inputs to the excitatory and the inhibitory populations, and c_1, c_2, c_3, c_4 are the strengths of connections between the populations. Notice that the values E and I may be negative, which means that the activity of the network is lower than that of the background activity.

A two-parameter bifurcation analysis of equation (1) with P and c_3 as control parameters (Borisyuk and Kirillov, 1992) showed a variety of non-trivial phase portraits and bifurcations. These bifurcations include, in particular, fold, Andronov–Hopf, fold points for limit cycles and homoclinic bifurcation (Ermentrout and Cowan, 1979). Moreover, several higher codimension singularities have been demonstrated as well, such as Bogdanov–Takens and cusp singularities. From the variety of phase portraits we shall employ here only those where an unstable equilibrium is surrounded by a stable limit cycle (see Fig. 3.7 in Borisyuk and Kirillov (1992)). For the remainder of the paper we fix parameters of the single oscillator at the following values: $\theta_e = 4$, $b_e = 1.3$, $\theta_i = 3.7$, $b_i = 2.0$, $c_1 = 16$, $c_2 = 12$, $c_3 = 15$, $c_4 = 3$, $P = 1.5$ and $Q = 0$. Notice that the amplitude and period of oscillations may vary significantly in the corresponding region of the bifurcation diagram. However, for the parameter values given above, we remain far away from the critical boundaries where these significant changes can occur. Therefore, we can now build a network based on a neural oscillator with reliable oscillatory properties.

2.2. *A model of two interacting neural oscillators.* Consider two identical neural oscillators given by (1) and coupled using terms that may be interpreted as an additional external input. This system of coupled oscillators has the form (Borisyuk *et al.*, 1992b; Khibnik *et al.*, 1992):

$$\begin{aligned}
dE_1/dt &= -E_1 + (k_e - E_1)\cdot S_e(c_1E_1 - c_2I_1 + P + P_{12}),\\
dI_1/dt &= -I_1 + (k_i - I_1)\cdot S_i(c_3E_1 - c_4I_1 + Q + Q_{12}),\\
dE_2/dt &= -E_2 + (k_e - E_2)\cdot S_e(c_1E_2 - c_2I_2 + P + P_{21}),\\
dI_2/dt &= -I_2 + (k_i - I_2)\cdot S_i(c_3E_2 - c_4I_2 + Q + Q_{21}),
\end{aligned} \tag{2}$$

where

$$P_{12} = \alpha_1E_2 - \alpha_2I_2,\ P_{21} = \alpha_1E_1 - \alpha_2I_1,$$
$$Q_{12} = \alpha_3E_2 - \alpha_4I_2,\ Q_{21} = \alpha_3E_1 - \alpha_4I_1.$$

Here E_1, I_1 and E_2, I_2 describe activities of the first and the second oscillators, respectively. The terms P_{12}, P_{21}, Q_{12}, Q_{21} describe connections between the

oscillators, and coefficients α_1, α_2, α_3, α_4 represent the strength of the connections between subpopulations related to different oscillators. Since we have symmetric coupling of identical oscillators, equation (2) has the reflection symmetry of interchange of two oscillators.

We consider four types of (oriented) connections between oscillators in our neural network model (2).

(1) Connections between the excitatory populations:

$$P_{12}=\alpha_1 E_2,\ P_{21}=\alpha_1 E_1,\ Q_{12}=Q_{21}=0, \tag{3}$$

where α_1 is the control parameter.

(2) Connections from the inhibitory population of one oscillator to the excitatory population of the other oscillator:

$$P_{12}=-\alpha_2 I_2,\ P_{21}=-\alpha_2 I_1,\ Q_{12}=Q_{21}=0, \tag{4}$$

where α_2 is the control parameter.

(3) Connections from the excitatory population of one oscillator to the inhibitory population of the other oscillator:

$$P_{12}=P_{21}=0,\ Q_{12}=\alpha_3 E_2,\ Q_{21}=\alpha_3 E_1, \tag{5}$$

where α_3 is the control parameter.

(4) Connections between the inhibitory populations:

$$P_{12}=P_{21}=0,\ Q_{12}=-\alpha_4 I_2,\ Q_{21}=-\alpha_4 I_1, \tag{6}$$

where α_4 is the control parameter.

In principle, all these connections may be active simultaneously. However, in this paper we consider these connections individually and analyse how the dynamics of a neural network is affected by each of the connections separately. In particular, we assume that only one of the parameters α_j, $j=1, 2, 3, 4$, is non-zero at any instance.

For each case, we analyse how the different types of oscillatory regimes evolve under variation of the strength of the corresponding connections, and in particular, how their stability properties change. In sections 4–7 we present the detailed bifurcation diagram for each connection type and emphasize the evolution of the observable oscillatory regimes in the neural network.

3. Oscillatory Regimes and Their Bifurcations. In this section we focus on dynamical regimes of the neural network that show periodic activity of each neural population. These regimes are associated with limit cycles, or periodic orbits, in the phase space of equation (2). We suggest a classification of limit cycles that take into account the symmetry of the equation. We give particular

attention to the case of weak coupling. A brief review of possible limit cycle bifurcations that may be encountered under variation of the strength of connections is given in the Appendix. We refer the reader to the Appendix for the terminology used in the discussion of bifurcation diagrams.

3.1. *Classification of oscillatory regimes.* The symmetry of system (2) implies that any periodic solution can be classified as Symmetric limit cycle (**SC**), Antisymmetric limit cycle (**AC**), and Nonsymmetric limit cycle (**NC**). They are defined as follows.

Let $(\tilde{E}_1(t), \tilde{I}_1(t), \tilde{E}_2(t), \tilde{I}_2(t))$ be a periodic solution: $\tilde{E}_1(t) \equiv \tilde{E}_1(t+T)$, $\tilde{I}_1(t) \equiv \tilde{I}(t+T)$, $\tilde{E}_2(t) \equiv \tilde{E}_2(t+T)$, $\tilde{I}_2(t) \equiv \tilde{I}_2(t+T)$, where T is a (minimal) period. A symmetric limit cycle is such that $\tilde{E}_1(t) \equiv \tilde{E}_2(t)$, $\tilde{I}_1(t) \equiv \tilde{I}_2(t)$. It corresponds to *in-phase*, or synchronous, oscillations of populations of the excitatory and of the inhibitory neurons, respectively (Fig. 1a).

The antisymmetric limit cycle is such that $\tilde{E}_1(t+T/2) \equiv \tilde{E}_2(t)$, $\tilde{I}_1(t+T/2) \equiv \tilde{I}_2(t)$. This corresponds to *anti-phase* oscillations as the phase shift between the oscillators is equal to $T/2$ (Fig. 1b).

A limit cycle which is neither symmetric nor antisymmetric is called nonsymmetric. Due to the symmetry of system (2) the nonsymmetric limit cycles always exist in pairs: $(E_1, I_1, E_2, I_2) = (\tilde{E}_1(t), \tilde{I}_1(t), \tilde{E}_2(t), \tilde{I}_2(t))$ and $(E_1, I_1, E_2, I_2) = (\tilde{E}_2(t), \tilde{I}_2(\tilde{E}_1(t), \tilde{I}_1(t))$ (Fig. 1c). For a nonsymmetric limit cycle, the phase shift is generally a nonconstant function of parameters. This type of oscillations is called *out-of-phase* oscillations.

We shall extend the usage of the terminology "symmetric", "antisymmetric", and "nonsymmetric" to any invariant set of system (2) (equilibrium, limit cycle, invariant torus, chaotic attractor). Let Π be the reflection actin, as $\Pi(E_1, I_1, E_2, I_2) = (E_2, I_2, E_1, I_1)$. Consider a symmetry plane L defined as $E_1 = E_2$, $I_1 = I_2$. Note that it is invariant both under the flow of (2) and under reflection Π. An invariant set M of system (2) is called symmetric if $M \subset L$, antisymmetric if $M \cap L = \emptyset$ and $\Pi(M) = M$, and nonsymmetric if $\Pi(M) \neq M$.

Obviously, in a four-dimensional phase space of system (2) one can fit the following objects: symmetric and nonsymmetric equilibria; symmetric, antisymmetric and nonsymmetric limit cycles; antisymmetric and nonsymmetric 2-tori; nonsymmetric 3-torus; antisymmetric and nonsymmetric chaotic attractors. We shall see in the next sections that all these objects really appear in model (2), with the exception of a 3-torus which was not observed in our simulations. Obviously, non-symmetric objects should appear in symmetric pairs (M_1, M_2), where $M_2 = \Pi(M_1)$.

Quasiperiodic motions on a 2-torus are called *anti-phase envelope* or *out-of-phase envelope* oscillations, if the torus is antisymmetric or nonsymmetric, respectively. We can draw some similarity between anti-phase periodic oscillations and anti-phase envelope oscillations based on the following

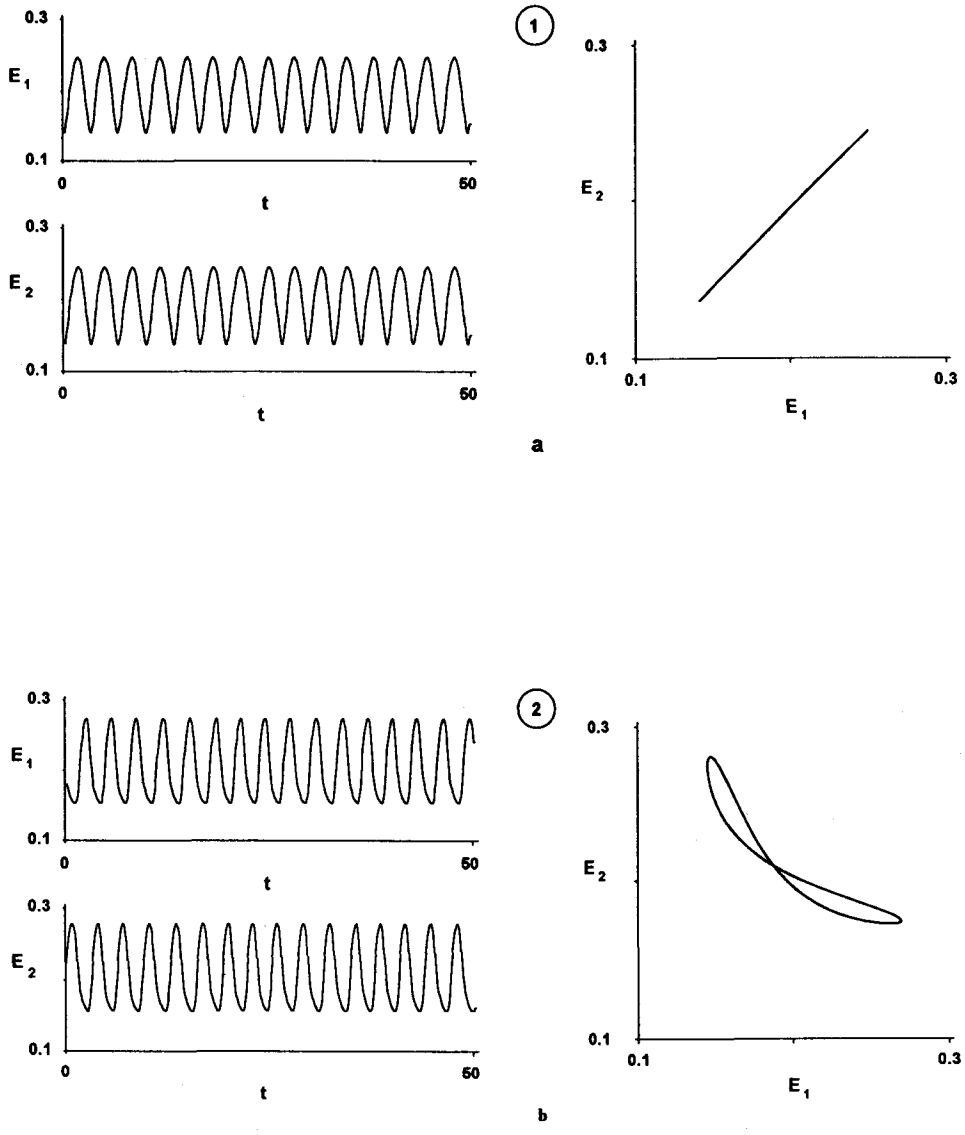

Figure 1. (a) and (b).

characteristic property. Let $\phi = \phi(x)$, $x = (E_1, I_1, E_2, I_2)$, be a function symmetric with respect to reflection Π, $\Pi \circ \phi(x) = \phi \circ \Pi(x)$ (e.g. $\phi = E_1 + E_2$). Comparing the frequencies of $\phi(t)$ and $x(t)$ in case of periodic oscillations, or corresponding envelope frequencies in case of quasiperiodic oscillations, we note that the first frequency is twice the second.

Remark that if oscillators are engaged in a symmetric or antisymmetric

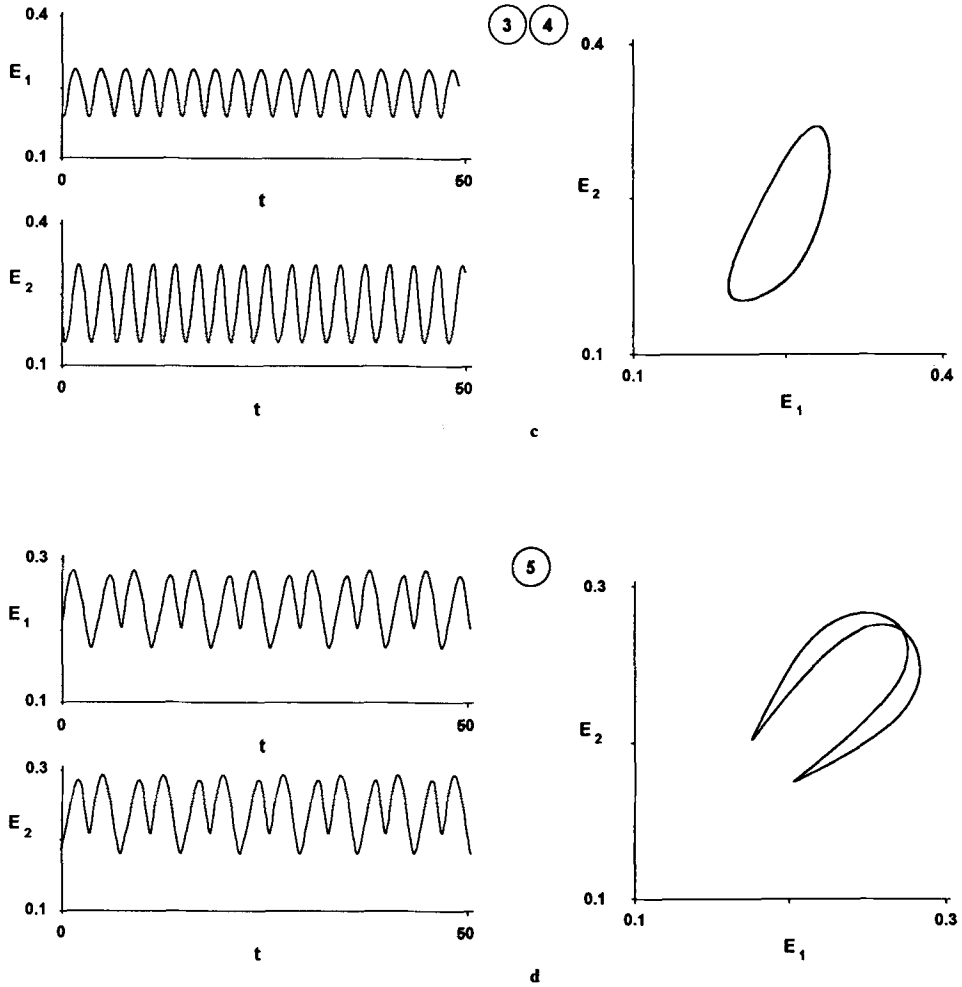

Figure 1. (c) and (d).

Figure 1. Examples of different types of periodic solutions (limit cycles). (a) Symmetric limit cycle **SC** (excitatory→inhibitory connections, $\alpha_3 = 1$). (b) Antisymmetric limit cycle **AC** (excitatory→excitatory connections, $\alpha_1 = 0.1$). (c) Nonsymmetric limit cycle **NC** (excitatory→excitatory connections, $\alpha_1 = 1.4$). (d) Antisymmetric limit cycle near its birth at period doubling bifurcation (inhibitory→excitatory connections, $\alpha_2 = 1.4$).

regime, they cannot be distinguished from each other while in a nonsymmetric regime they can.

A nice feature of any symmetric equilibrium or limit cycle is that its stability can be characterized separately with respect to symmetric and nonsymmetric perturbations. For this we use the notation (q, r), where q show the stability in

L, r shows the stability with respect to perturbations transversal to L, and q, r is either "$-$" meaning stable, or "$+$", meaning unstable.

3.2. *Weak coupling.* We start with the case $\alpha_j = 0$, for which system (2) describes two identical and uncoupled oscillators. The two-dimensional phase space of each oscillator contains an unstable equilibrium **O** and a stable limit cycle **C**. The phase space of system (2) appears as a product of these phase spaces of the uncoupled oscillators. This "product" structure implies the existence of the following invariant sets:

- symmetric equilibrium $\mathbf{SE} = \mathbf{O} \times \mathbf{O} (\mathbf{SE} \in \mathbf{L})$;
- two nonsymmetric limit cycles $\mathbf{NC}_1 = \mathbf{C} \times \mathbf{O}$ and $\mathbf{NC}_2 = \mathbf{O} \times \mathbf{C}$, forming a symmetric pair; and
- antisymmetric invariant 2-torus $\mathbf{T} = \mathbf{C} \times \mathbf{C}$.

The equilibrium **SE** is absolutely unstable (all four eigenvalues lie in the positive halfplane). The limit cycles $\mathbf{NC}_1$ and $\mathbf{NC}_2$ are of saddle type (one multipler lies inside and two others lie outside the unit circle). The 2-torus **T** is stable. The above stability properties follow from the stability of **C** and the instability of **O**. The 2-torus **T** consists of a continuum of periodic orbits as we can choose an arbitrary phase shift φ, $0 \leqslant \varphi < T$, between the oscillators. Note that the 2-torus contains the symmetric periodic orbit **SC**, with zero phase shift $\varphi = 0$, and the antisymmetric periodic orbit **AC**, with $\varphi = T/2$. Other priodic orbits on **T** are nonsymmetric (**NC**-type). They are different, however, from periodic orbits $\mathbf{NC}_1$ and $\mathbf{NC}_2$; the latter are obtained as a product of an equilibrium and a period orbit and obviously are planar, which means that one oscillator stays in a quiescent mode.

We now perturb α_i assuming $0 < \alpha_j \ll 1$. Structural stability of the equilibrium **SE** and the limit cycles $\mathbf{NC}_1$, $\mathbf{NC}_2$ implies that they persist under perturbations and preserve their stability type. The 2-torus **T** also persists due to its normal hyperbolicity (Fenichel, 1971), although the dynamics on it changes (i.e. it is structurally unstable). Typically, on the perturbed 2-torus **T**, only a finite (and even) number of periodic orbits "surive". In particular, the symmetric and antisymmetric periodic orbits **SC** and **AC** survive and remain on the torus due to their symmetric properties; note that **SC** has $(-, \cdot)$ stability type. We have shown, using perturbation techniques (Malkin, 1956; Cymbalyuk *et al.*, 1994; Ermentrout and Kopell, 1991) that no nonsymmetric periodic orbits survive on **T**, for connections of any type (1)–(4). To do that, we computed numerically a certain integral $H(\varphi)$ over the original periodic orbit **C**, where φ is a phase shift, $0 \leqslant \varphi < T$, and verified that it has only two zeros, at $\varphi = 0$ and $\varphi = T/2$, corresponding to orbits **SC** and **AC**, respectively. The stability of these orbits on the torus is defined by the sign of $\partial H / \partial \varphi$ at the corresponding roots. For different connection types we computed the following stability of **SC** and **AC**:

(1) Excitatory to excitatory: **AC** is stable, **SC** is unstable.

(2) Inhibitory to excitatory: **SC** is stable, **AC** is unstable.
(3) Excitatory to inhibitory: **SC** is stable, **AC** is unstable.
(4) Inhibitory to inhibitory: **AC** is stable, **SC** is unstable.

Note that instability of **SC** means that it has $(-, +)$ type. We summarize that for inhibitory to excitatory and for excitatory to inhibitory connections the in-phase mode is stable. For the remaining two connection types this mode appears unstable but then the anti-phase mode is stable. Note that these results are limited to the case of weak coupling. In the next four sections we shall describe, for each connection type, what happens when the coupling becomes stronger. We find a change of stability for in-phase and the anti-phase modes, the emergence of new oscillatory modes, even more complicated dynamics or oscillatory death meaning that no stable oscillatory mode exists.

4. Two Oscillators with Connections between Excitatory Neuronal Populations. For the case of connections between the excitatory neuronal populations, a schematic bifurcation diagram for system (2) with connection terms (3) and α_1 as a control parameter is presented in Fig. 2.

Symmetric equilibrium ***SE***. For $\alpha_1 = 0$, **SE** has stability type $(+, +)$. Increasing α_1, the equilibrium undergoes Andronov–Hopf bifurcation twice, at point $B(\alpha_1 = 0.50)$ and point $H(\alpha_1 = 5.573)$ and become stable; the corresponding transition is $(+, +) \to (-, +) \to (-, -)$ with branches of antisymmetric and symmetric limit cycles emerging at points B and H. Note that both bifurcations are backward and supercritical (see the Appendix for definitions). Two fold bifurcations occur inside the symmetry plant at points $I(\alpha_1 = 5.574)$ and $J(\alpha_1 = 5.333)$. In the interval (J, I) three symmetric equilibria exist simultaneously: two of them are stable, and the third one is a saddle with one positive eigenvalue (it has type $(+, -)$).

Symmetric limit cycle ***SC***. For small α_1 the limit cycle **SC** is unstable, of type $(-, +)$. It becomes stable at a (subcritical) symmetry-breaking bifurcation point $D(\alpha_1 = 1.72)$, giving rise to two saddle nonsymmetric limit cycles $\mathbf{NC}_3$ and $\mathbf{NC}_4$, for $\alpha^1 > D$. The limit cycle **SC** remains stable until α_1 reaches point $F(\alpha_1 = 5.34)$ when it disappears on a homoclinic orbit associated with the symmetric saddle mentioned above. Approaching point F (not shown in the picture), the period of the stable in-phase oscillations grows logarithmically fast to infinity. Another small branch of symmetric limit cycles exists between points $K(\alpha_1 = 5.5711)$ and H; at point K (not shown in the picture) we have another homoclinic orbit, similar to the previous one. It is worth noting that under a perturbation of the model two such close homoclinic points can easily merge and annihilate; to simplify the picture, it is natural to assume that the branch **SC** continues until it terminates at point H.

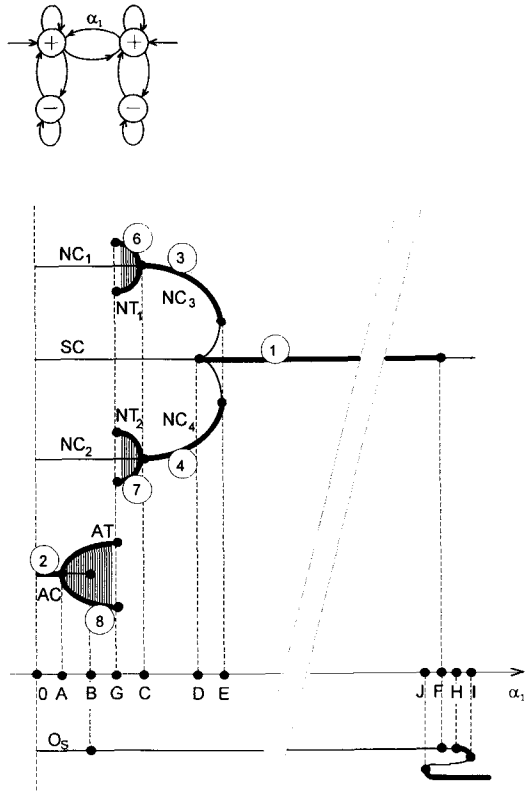

Figure 2. Schematic bifurcation diagram for excitatory→excitatory connections. Note that the system displays quasiperiodic (envelope) oscillations in a large parameter range. Stable regimes are drawn by bold and unstable by thin curves. **SE**–symmetric equilibrium, **NE**–nonsymmetric equilibrium, **SC**–symmetric limit cycle, **AC**–antisymmetric limit cycle, **NC**–nonsymmetric limit cycle, **AT**–antisymmetric torus, **NT**–nonsymmetric torus.

Antisymmetric limit cycle AC. The limit cycle **AC** is stable for small α_1 and moreover it appears to be the only attractor in the system. At point $A(\alpha_1 = 0.25)$ this limit cycle loses stability via a torus bifurcation and a stable antisymmetric torus, denoted **AT**, emerges for $\alpha_1 > A$ (see Fig. 3b). The unstable limit cycle **AC**, merges with equilibrium **SE** at point B when the latter undergoes the Andronov–Hopf bifurcation described above.

Nonsymmetric limit cycles NC_1 and NC_2. The limit cycles $\mathbf{NC}_1$ and $\mathbf{NC}_2$ are of saddle type, for small α_1. They gain stability at point $C(\alpha_1 = 1.02)$ via a (backward) torus bifurcation, by merging with a pair of stable nonsymmetric tori $\mathbf{NT}_1$ and $\mathbf{NT}_2$ (see Fig. 3a), respectively. Increasing α_1 further, the stable nonsymmetric limit cycles $\mathbf{NC}_1$ and $\mathbf{NC}_2$ (pairwise) collide with the saddle

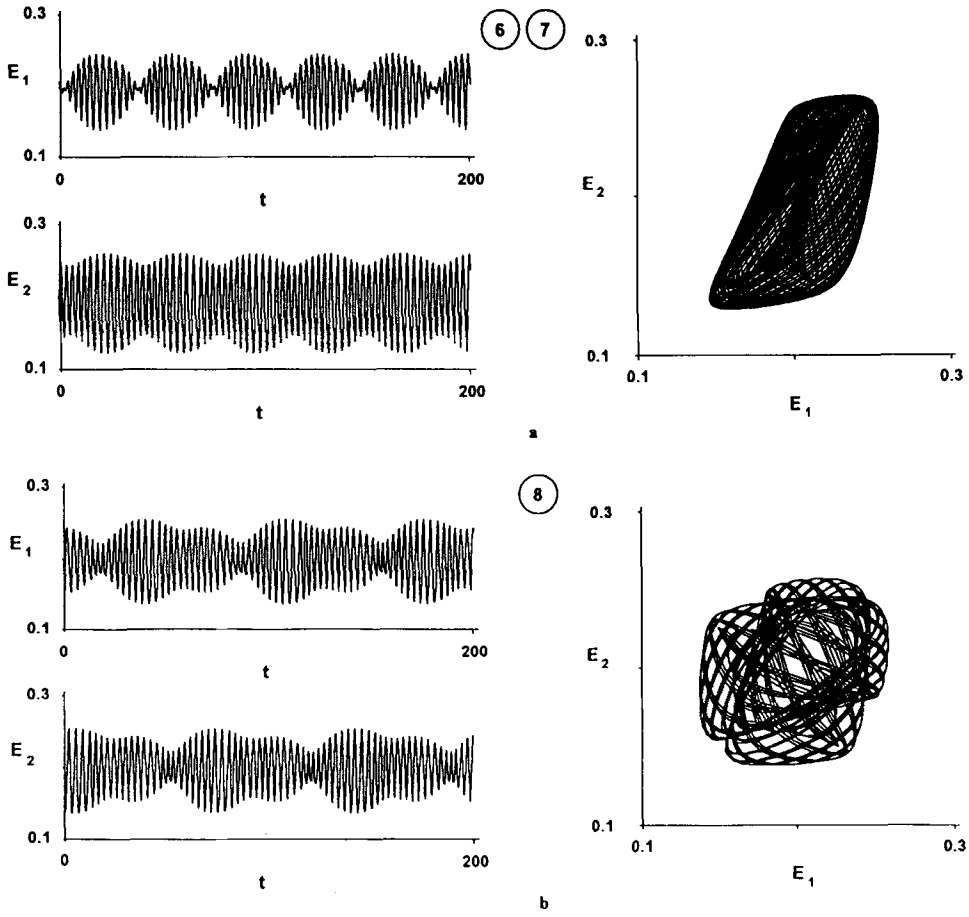

Figure 3. Example of envelope oscillations (2-tori). (a) Nonsymmetric torus **NT** (excitatory→excitatory connections, $\alpha_1 = 0.85$). (b) Antisymmetric torus **AT** (excitatory→excitatory connections, $\alpha_1 = 0.5$).

nonsymmetric limit cycles $\mathbf{NC}_3$ and $\mathbf{NC}_4$ at point E ($\alpha_1 = 1.76$), a fold bifurcation of limit cycles.

Antismmetric torus ***AT*** *and nonsymmetric tori* $\boldsymbol{NT}_1$ *and* $\boldsymbol{NT}_2$ (Figs 3 and 4). In the interval (A, C) no stable limit cycles exist, only the tori are stable. In numerical simulations we observe two subintervals, (A, G) and (G, C), such that the first one carries one antisymmetric torus **AT**, linked to **AC**, and the second one carries two nonsymmetric tori $\mathbf{NT}_1$ and $\mathbf{NT}_2$, linked to $\mathbf{NC}_1$ and $\mathbf{NC}_2$, respectively. At point $G(\alpha_1 = 0.6910\ldots)$ **AT** "transforms" into $\mathbf{NT}_1$ and $\mathbf{NT}_2$; we call this phenomenon a *torus symmetry breaking*. Numerical experiments provide quite strong evidence that this transition involves homoclinicity associated with the symmetric limit cycle **SC**. This suggests that

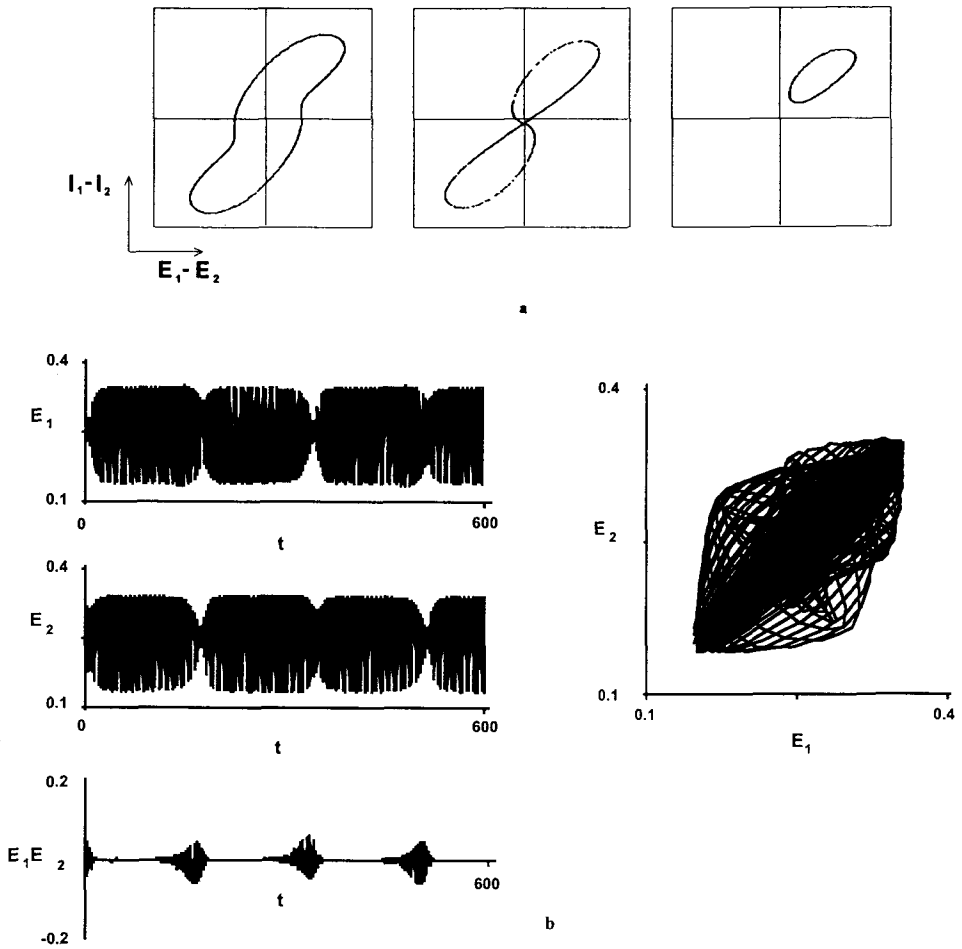

Figure 4. Torus-symmetry-breaking bifurcation in the case of excitatory→ excitatory connections. (a) Poincare sections for $\alpha_1=0.5$, $\alpha_1=0.691$, $\alpha_1=0.85$. Secant plane: $E_1+E_2=0.44$. (b) Anti-phase envelope oscillations for $\alpha_1=0.691$. Note the substantial growth of the envelope period compared to that in Fig. 3.

the phenomenon can also be called a *torus gluing bifurcation*, as the underlying mechanism is similar to a gluing bifurcation for periodic orbits (Gambaudo *et al.*, 1988).

Figure 4 illustrates the torus symmetry breaking bifurcation using the Poincaré map and the related time series. In Fig. 4a we plot the Poincaré map on plane $E_1+E_2=\text{const}$. The left graph, computed for $\alpha_1<G$, shows one closed invariant curve which is apparently symmetric with respect to the origin; the symmetry implies that the corresponding torus is antisymmetric. Note that the origin is a saddle fixed point corresponding to the symmetric limit cycle **SC**. The right graph, computed for $\alpha_1>G$, displays one of two symmetrically

located invariant curves; each of them represents one nonsymmetric torus. Approaching point G from the left, the symmetric invariant curve gets closer to the origin, as shown in the middle picture, and eventually blows up forming two separated closed curves. We conjecture that the torus symmetry breaking bifurcation is closely related to the appearance of a homoclinic orbit to the saddle symmetric limit cycle **SC**. Apparently, due to the symmetry of the system, two homoclinic orbits should arise simultaneously. We also note that probably the torus symmetry breaking appears not to be a single bifurcation but a complicated transition sequence involving a homoclinic invariant set and associated chaotic dynamics; the fact that we have not observed these phenomena in the model means only that the corresponding parameter interval may be extremely small (see also discussion in Khibnik *et al.*, 1992).

Near the torus symmetry breaking bifurcation point the coupled oscillators look synchronized most of the time (Fig. 4b). Indeed, the related orbit comes very close to the symmetric limit cycle and traces it for a rather long time. Due to the phase instability of **SC**, however, this cannot last forever, and the orbit necessarily leaves neighborhood of **SC**, developing a substantial phase shift. Soon, it "flies back" to **SC** meaning that the phase shift decays to zero again. This demonstrates the alternation of (approximately) in-phase and out-of-phase oscillations. Clearly, the in-phase oscillations occur most of the time.

Remark. The torus gluing bifurcation of the type described above (we shall see still another type in section 6) appears in the context of the loss of stability of limit cycles near a 1:2 resonance, codimension two bifurcation phenomenon if no symmetry is imposed (Arnold, 1983). We are not aware of any mathematical literature studying torus gluing, neither in this nor in a different context. For other examples of torus gluing, of essentially the same type, we refer to Aronson *et al.* (1990) and Skeldon (1994).

We now summarize the observed picture of bifurcations, emphasizing only the *stable* oscillatory regimes and how they evolve when α_1 grows.
$(0, A)$: Anti-phase periodic oscillations.
(A, G): Anti-phase envelope oscillations.
(G, C): Out-of-phase envelope oscillations.
(C, D): Out-of-phase periodic oscillations.
(D, E): In-phase and out-of-phase periodic oscillations.
(E, H): In-phase periodic oscillations.
$\alpha_1 > H$: Oscillatory death.

5. Two Osillators with Connections from the Inhibitory Population to the Excitatory One. Consider connections from the inhibitory to the excitatory neuronal populations described by the connection terms (4) with α_2 as a control parameter. The related bifurcation diagram is presented in Fig. 5. Note

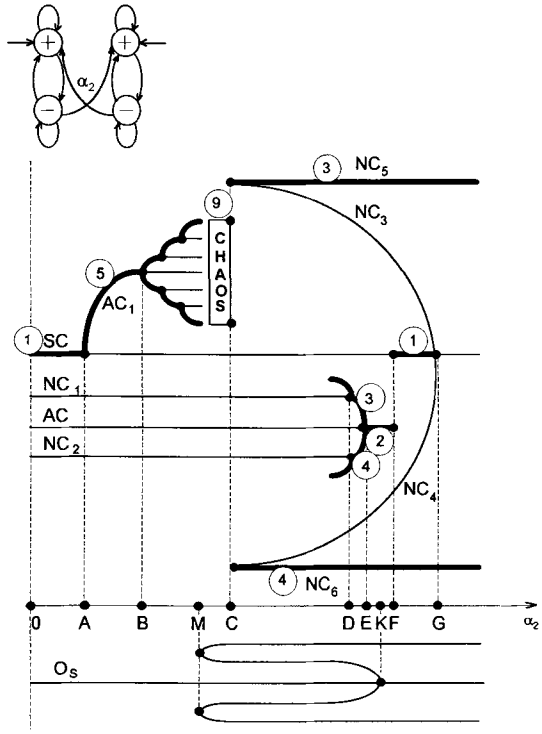

Figure 5. Schematic bifurcation diagram for inhibitory→excitatory connections. Increasing α_2, chaos arises via a cascade of period doublings and disappears via an intermittency phenomenon.

that this type of connections shows the most complicated picture of bifurcations, particularly involving the development of chaotic behavior.

Symmetric equilibrium ***SE***. Recall that **SE** is completely unstable for $\alpha_2 = 0$. When α_2 increases, the stability type changes from $(+, +)$ to $(+, -)$ at the symmetry breaking bifurcation point $K(\alpha_2 = 5.35)$. Two nonsymmetric saddle equilibria, merging with **SE** at K, collide with another pair of nonsymmetric equilibria at the fold bifurcation point M $(\alpha_2 = 2.87)$. These latter equilibria exist for $\alpha_2 > M$.

Symmetric limit cycle ***SC***. For zero and small α_2, limit cycle **SC** is stable. At point $A(\alpha_2 = 1.16)$ it loses stability, changing from $(-, -)$ to $(-, +)$. A period doubling bifurcation at point A leads to the birth, for $\alpha_2 > A$, of a stable antisymmetric limit cycle, denoted **AC**′, the period of which is approximately twice the period of **SC** (Fig. 1d). Notice that antisymmetric limit cycles **AC**′ and **AC** form different branches; as we shall see further, **AC**′ gives birth to a cascade of bifurcations leading to chaos.

At point $F(\alpha_2 = 5.46)$, the limit cycle **SC** becomes stable again, via the (backward) period doubling bifurcations. The emerging limit cycle with doubled period exists for $\alpha_2 < F$ and appears to be stable and antisymmetric; in fact that is **AC**. The limit cycle **SC** is stable between points F and $G(\alpha_2 = 5.98)$; at the latter point it undergoes the (subcritical) symmetry breaking bifurcation, tranforming again into $(-, +)$ type and giving birth to two saddle nonsymmetric limit cycles $\mathbf{NC}_3$ and $\mathbf{NC}_4$ for $\alpha_2 < G$.

Antisymmetric limit cycle AC. For small values of α_2, the limit cycle **AC** is unstable. It becomes stable at point $E(\alpha_2 = 5.03)$ when the (backward) symmetry breaking bifurcation occurs that gives rise to a pair of stable nonsymmetric limit cycles for $\alpha_2 < E$ (actually these are $\mathbf{NC}_1$ and $\mathbf{NC}_2$). Then **AC** approaches the symmetric limit cycle **SC** and merges with it at point F.

Nonsymmetric limit cycles NC_1 and NC_2. The limit cycles $\mathbf{NC}_1$ and $\mathbf{NC}_2$ are unstable for small α_2. Each of them becomes stable at point $D(\alpha_2 = 4.99)$ via the (backward) period doubling bifurcation, by merging with a nonsymmetric limit cycle with the doubled period. Both limit cycles $\mathbf{NC}_1$ and $\mathbf{NC}_2$ approach each other and merge with the antisymmetric limit cycle **AC** at point E (see above).

Other limit cycles. Consider the stable antisymmetric limit cycle $\mathbf{AC}_1$ which has appeared at point A. When α_2 increases, it loses stability at point $B(\alpha_2 = 1.90)$ via the (supercritical) symmetry breaking bifurcation which gives birth to a pair of stable nonsymmetric limit cycles. These cycles in turn become unstable at $\alpha_2 = 1.94$ via a (first) period doubling bifurcation. A cascade of period doubling bifurcations than follows culminating in the appearance of two nonsymmetric chaotic attractors (Fig. 6a).

When α_2 increases, the symmetric pair of unstable nonsymmetric limit cycles $\mathbf{NC}_3$ and $\mathbf{NC}_4$ appears at point $C(\alpha_2 = 3.27)$, together with the other symmetric pair of stable limit cycles $\mathbf{NC}_5$ and $\mathbf{NC}_6$, when the system undergoes a fold bifurcation for limit cycles. At point C, we have two nonsymmetric saddle-node limit cycles created by collision of $\mathbf{NC}_3$ and $\mathbf{NC}_5$ ($\mathbf{NC}_4$ and $\mathbf{NC}_6$, respectively). The stable limit cycles $\mathbf{NC}_5$ and $\mathbf{NC}_6$ persist for all $\alpha_2 > C$, while the unstable limit cycles $\mathbf{NC}_3$ and $\mathbf{NC}_4$ merge with limit cycle **SC** at point G. The fold bifurcation at point C has, however, some additional global features playing a crucial role in the death of chaos, which will be discussed below.

Chaotic attractors (Fig. 6). A pair of chaotic attractors arise via a period doubling cascade of nonsymmetric limit cycles, which makes these attractors nonsymmetric also. Shortly after they arise, these two attractors "merge" into a single antisymmetric chaotic attractor. This attractor exists until α_2 reaches

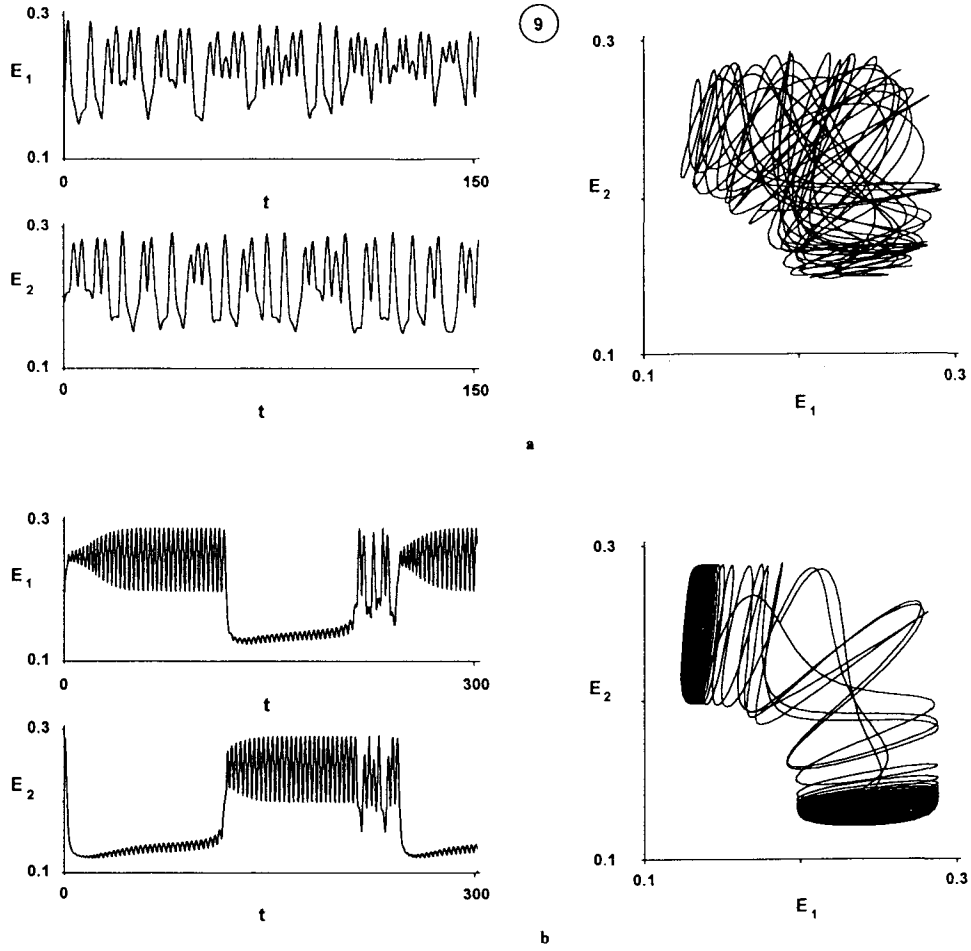

Figure 6. Chaotic oscillations in the case of inhibitory→excitatory connections. (a) $\alpha_2 = 2.5$; (b) $\alpha_2 = 3.25$—intermittency.

point C where a pair of saddle-node nonsymmetric limit cycles arise, and then it dies. This observation reveals global consequences of the fold bifurcation occurring at point C. Indeed, as parameter α_2 approaches C, an orbit on the chaotic attractor tends to remain longer and longer near the two locations in the phase space where the saddle-node limit cycles will appear. As the orbit arrives at either of these locations, the oscillations become nearly periodic. Therefore, we observe near point C an intermittency phenomenon: both oscillators run almost periodically in time, switching rarely but randomly between regimes where either the first or the second oscillators dominates (Fig. 6b).

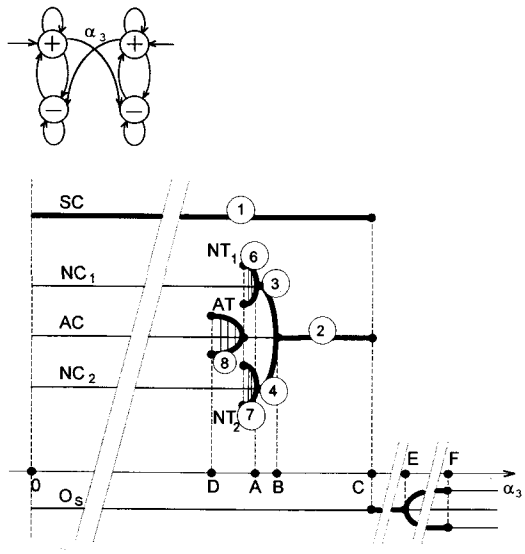

Figure 7. Schematic bifurcation diagram for excitatory→inhibitory connections. Double Hopf bifurcation at point C leads to the appearance of two stable regimes: symmetric and antisymmetric limit cycles. Their basins of attraction are separated by an invariant torus of saddle type, also born at C.

We conclude our analysis of inhibitory→excitatory connections with the following bifurcation picture for stable regimes.
$(0, A)$: In-phase periodic oscillations.
(A, B): Anti-phase periodic oscillations.
(B, C): Transition to chaos via the period doubling cascade and chaotic oscillations.
(C, D): Out-of-phase periodic oscillations.
(D, E): Out-of-phase periodic oscillations (two different profiles).
(E, F): Anti-phase and out-of-phase periodic oscillations.
(F, G): In-phase and out-of-phase periodic oscillations.
$\alpha_2 > G$: Out-of-phase periodic oscillations.

6. Two Oscillators with Connections from the Excitatory Population to the Inhibitory One. Consider now connections from the excitatory to the inhibitory neuronal populations, i.e. system (2) with the connection terms (5) and with α_3 as a control parameter. We obtain the bifurcation diagram shown in Fig. 7.

Symmetric equilibrium ***SE.*** When α_3 increases, the stability type of **SE** changes from $(+, +)$ to $(-, -)$ at point $C(\alpha_3 = 2.49)$, i.e. the completely unstable equilibrium becomes immediately stable. At this point we have

simultaneously two Hopf pairs of eigenvalues. Note that this usually happens at a codimension two phenomenon, but for this connection type (more generally, for any connections with $\alpha_1 = \alpha_4 = 0$) it becomes a one-parameter bifurcation. Using normal form computations (see Guckenheimer and Holmes, 1983) we show that three invariant sets bifurcate from **SE** simultaneously for $\alpha_3 < C$: two stable limit cycles—symmetric and antisymmetric (**SC** and **AC**)—and a saddle antisymmetric torus **AT'**. The torus is difficult to compute by direct integration, since it is unstable both in forward and in backward time. Nonetheless, in simulations one can easily visualize the torus as a long-term transient pattern and observe the envelope oscillations of anti-phase type. At point $E(\alpha_3 = 7.43)$ of symmetry breaking bifurcation, **SE** changes stability to $(-, +)$ type, giving rise to two stable nonsymmetric equilibria (they, in turn, undergo Andronov–Hopf bifurcation at $F(\alpha_3 = 13.15)$ where two nonsymmetric limit cycles appear).

*Symmetric limit cycle **SC**.* The limit cycle **SC** is stable on the whole interval $(0, C)$. At point C it merges with equilibrium **SE**, as described above.

*Antisymmetric limit cycle **AC**.* Being unstable for small values of α_3, limit cycle **AC** gains stability at point the (backward) symmetry breaking bifurcation $B(\alpha_3 = 1.67)$. Two stable nonsymmetric limit cycles $\mathbf{NC}_1$ and $\mathbf{NC}_2$ appear at this point for $\alpha_3 < B$. At point C limit cycle **AC** merges with equilibrium **SE**.

Nonsymmetric limit cycles $\mathbf{NC}_1$ and $\mathbf{NC}_2$. Limit cycles $\mathbf{NC}_1$ and $\mathbf{NC}_2$ are unstable for small α_3. They become stable at the (backward) torus bifurcation point $A(\alpha_3 = 1.59)$, where the stable tori $\mathbf{NT}_1$ and $\mathbf{NT}_2$, existing for $\alpha_3 < A$, shrink to $\mathbf{NC}_1$ and $\mathbf{NC}_2$, respectively. At point B these limit cycles merge with limit cycle **AC**, as described above.

*Antisymmetric torus **AT** and nonsymmetric tori $\mathbf{NT}_1$ and $\mathbf{NT}_2$.* Tori $\mathbf{NT}_1$ and $\mathbf{NT}_2$ bifurcate from $\mathbf{NC}_1$ and $\mathbf{NC}_2$ respectively, and almost immediately glue into the antisymmetric torus **AT**. This appears to be similar to the gluing bifurcation described in section 4, but there are some differences. The similarity is that an envelope pattern corresponding to a torus contains a nearly periodic pattern, which gets longer and longer, with the envelope period going to infinity, when the parameters approach the gluing point. The difference is that we have here a periodic pattern resembling an antisymmetric limit cycle, as opposed to a symmetric limit cycle in the previous case. In other words, here the nonsymmetric tori approach and glue together on the antisymmetric limit cycle, while for the case of mutual excitatory connections a symmetric limit cycle is involved.

At point $D(\alpha_3 = 1.38)$ the antisymmetric torus **AT** collides with another

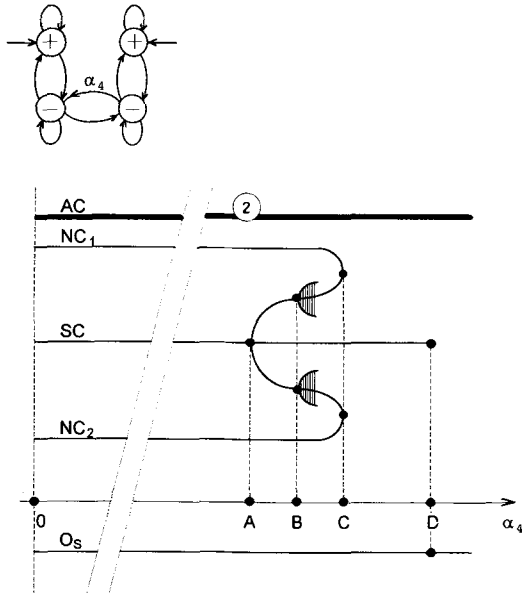

Figure 8. Schematic bifurcation diagram for inhibitory→excitatory connections. Antisymmetric limit cycle is the only stable regime in the whole parameter range.

antisymmetric torus **AT'** of saddle type. There is numerical evidence that this is the same torus as that bifurcated from **SE** at point C; we use this conjecture to complete the picture (Fig. 7).

The analysis of the excitatory→inhibitory connections is summarized in the following bifurcation scheme.

$(0, D)$: In-phase periodic oscillations.
(D, G): In-phase periodic and anti-phase envelope oscillations.
(G, A): In-phase periodic and out-of-phase envelope oscillations.
(A, B): In-phase and out-of-phase periodic oscillations.
(B, C): In-phase and anti-phase periodic oscillations.
(C, F): Oscillatory death.
$\alpha_3 > F$: Out-of-phase periodic oscillations.

7. Two Oscillators with Connections between Inhibitory Populations. In case the inhibitory populations are connected, the simplest bifurcation diagram appears (Fig. 8). Here the connection terms in system (2) are given by the expressions (6) and α_4 is treated as a control parameter.

*Symmetric equilibrium **SE**.* Being completely unstable for small α_4, **SE** changes to saddle type, $(-, +)$, at the (backward) Andronov–Hopf bifurcation point $D(\alpha_4 = 0.61)$. This bifurcation gives rise to a saddle symmetric limit cycle **SC** for $\alpha_4 < D$.

Symmetric limit cycle ***SC***. For all values of α_4 the symmetric limit cycle **SC** appears to be unstable, of $(-, +)$ type. At point $A(\alpha_4 = 0.49)$ it undergoes a symmetry breaking bifurcation leading to the appearance of a pair of saddle limit cycles $\mathbf{NC}_3$ and $\mathbf{NC}_4$ for $\alpha_4 > A$. At point D $(\alpha = 0.61)$ this limit cycle merges with the symmetric equilibrium **SE**.

Antisymmetric limit cycle ***AC***. For all values of α_4 the antisymmetric limit cycle is stable.

Nonsymmetric limit cycles $\boldsymbol{NC_1}$ *and* $\boldsymbol{NC_2}$. The limit cycles $\mathbf{NC}_1$ and $\mathbf{NC}_2$ are of saddle type for small α_4. At point $C(\alpha = 0.55)$ they pairwise collide with two other nonsymmetric, completely unstable limit cycles $\mathbf{NC}_3$ and $\mathbf{NC}_4$, in a fold bifurcation of limit cycles. Between points A and C, at point $B(\alpha_4 = 0.54)$, limit cycles $\mathbf{NC}_3$ and $\mathbf{NC}_4$ undergo a torus bifurcation which gives rise, for $\alpha_4 < B$, to two completely unstable nonsymmetric tori $\mathbf{NT}_1$ and $\mathbf{NT}_2$. They can easily be visualized in backward time.

Nonsymmetric tori $\boldsymbol{NT_1}$ *and* $\boldsymbol{NT_2}$. When α_4 decreases, the tori $\mathbf{NT}_1$ and $\mathbf{NT}_2$ are involved in quite complicated transitions (torus doubling, chaotic repeller). Ultimately, they die approaching a point where both $\mathbf{NC}_1$ and $\mathbf{NC}_2$ have a homoclinic orbit.

In the case of mutual inhibitory connections the picture of stable oscillatory regimes is trivial:

for all α_4: anti-phase periodic oscillations.

8. Summary and Discussion. In this paper, we considered an oscillatory neural network built upon coupled Wilson–Cowan neural oscillators, each describing the average activities of excitatory and inhibitory populations of neurons. We explored the capabilities of a rather simple neural network, consisting of neural oscillators, to exhibit different dynamical behavior. We focused primarily on the dependence of the dynamics of the entire network on the type and the strength of the connections between the neural oscillators.

We considered particular forms of coupling which, for a given oscillator, just add (weighted) output from one or more other oscillators to the external input of this oscillator. This is a *direct* coupling (Aronson *et al.*, 1990), which differs in many cases from *diffusive* coupling.

This choice has led to the model (2), which generally takes into account four connection types: excitatory to excitatory, inhibitory to excitatory, excitatory to inhibitory and inhibitory to inhibitory. In order the achieve a better

understanding of the role of each connection type in the dynamics of the network, we investigated each connection type separately. We believe that this approach forms a basis for further experiments with "mixed" connections.

Our study of model (2) revealed a great *variety* of dynamical regime, despite the simplicity of the two-oscillator neural network. Furthermore, by choosing different connection types and by varying the strength of the connections, we found qualitatively different network dynamics. This shows that the type and the strength of the connections play a crucial role. In this paper, we were in the first place concerned with the analysis of the influence of the connection type on the dynamics of the network.

We now summarize the most interesting features of the model. Afterwards we shall discuss how some particular oscillatory modes can be used for information processing.

Weak coupling. In case of a weak coupling, the model manifests either in-phase or anti-phase stable periodic oscillations. The anti-phase oscillations arise if we take purely excitatory or purely inhibitory connections. For two other types of connections, i.e. from excitatory to inhibitory to excitatory, we have synchronous (in-phase) oscillations. These observations allow us to suggest the following hypothesis: a weak coupling between "differently named" populations leads to a synchronizing effect (after a transient, oscillations become synchronous), while the coupling between "similarly named" populations leads to a desynchronizing effect (after a transient, the oscillators oscillate in an anti-phase fashion)—see also (Schillen and König, 1991; König and Schillen 1991; Ermentrout and Kopell, 1991).

"*Intermediate*" *coupling.* As the strength of the connection becomes larger, the dynamics of the network may change. Consider for example the case of excitatory to excitatory connections. First, the changes develop gradually: anti-phase periodic oscillations turn into envelope oscillations, whose envelope profile inherits the characteristic anti-phase pattern. Afterwards this pattern is destroyed which leads to out-of-phase envelope oscillations, and ultimately we arrive at out-of-phase periodic oscillations. Then an abrupt change occur: the system "jumps" from out-of-phase periodic oscillations to in-phase oscillations. The last transition is again smooth: the amplitude of the in-phase oscillations decays to zero, which results in a quiescent mode.

Note that for excitatory to inhibitory and for inhibitory to excitatory connections the scenario is different but similar in the sense that the strength of the connections considerably influences the dynamics of the network. However, in the case of inhibitory to inhibitory connections the dynamics does not change at all, i.e. no bifurcations involving stable regimes occur.

Multistability. We draw attention to the presence of several multistability regions in the model (2) (e.g. interval (D, E) in Fig. 2, where in-phase and out-of-phase regimes coexist). This is closely related to the possibility of a real

neural network to respond to a given signal in a non-unique way; the response depends upon initial data which could be difficult to control.

Evelope and chaotic oscillations. For weak coupling, we observe periodic oscillations, either in-phase or anti-phase. For strong coupling, we have either periodic oscillations of any of the three possible types, or oscillatory death. For intermediate coupling, however, we observe also quasiperiodic or chaotic behavior. Note that even for quasiperiodic and chaotic regimes some relationships between the phases of the oscillators may still occur (e.g. anti-phase envelope oscillations in Fig. 3b). Usually they can be detected by examining the symmetry of the attractor. Quasiperiodic oscillations were found in model (2) for excitatory to excitatory and for excitatory to inhibitory connections, and chaotic oscillations were observed for inhibitory to excitatory connections.

In case connections between *excitatory populations* (mutual excitation) exist, quasi-periodic oscillations occur for a reasonably wide range of connection strengths. For sufficiently large values of the connection strengths, the mutual excitatory connections lead to synchronous oscillations and then to oscillator death.

Connections from the *inhibitory population to the excitatory one* produce complex chaotic behavior. Note that two coupled neural oscillators are sufficient for demonstrating "random" behavior, but such a regime occurs only for one of the four considered types of connection. Note also that for a sufficiently large connection strength, the neural network exhibits out-of-phase periodic oscillations.

Connections from the *excitatory population to the inhibitory one* lead to a substantial region of multistability where synchronous and nonsynchronous oscillatory regimes exist simultaneously. Such multistable regimes can be used for modeling memory and attention functions (Borisyuk, 1991). Oscillator death and the restoration of out-of-phase oscillations are observed when the strength of coupling increases.

Connections between *inhibitory populations* (mutual inhibition) result in stable anti-phase oscillations for the whole parameter range. This is consistent with the behavior of many other oscillatory systems where mutual inhibition also leads to persistent anti-phase oscillations (see, e.g. Wang and Rinzel, 1993; Schutter *et al.*, 1993).

Finishing our discussion, let us discuss about the possible role and significance of chaotic and quasiperiodic oscillations for data processing in a brain. The advantages of chaotic behavior for brain functioning were considered by Nicolis (1990), Nicolis and Tsuda (1985), Tsuda (1992), Yao *et al.* (1991), Dmitriev (1993) and others. These papers focused on chaotic regimes in solving problems of pattern recognition, classification and memorization of information. An important feature of systems with chaotic dynamics, exploited

in many applications, is that they show easy transitions from chaos to a periodic oscillatory mode; this is caused by the fact that the frequency spectrum of chaotic behavior is a mixture of different frequencies of oscillations.

Envelope oscillations have not received much attention yet. We believe that envelope oscillations may help to resolve the following problem. It is known that frequency encoding of stimuli is impeded by insufficiency of information capacity. Indeed, the range of admissible frequencies is not large, and due to relatively low resolution in the frequency domain, it may not be easy to distinguish between different frequencies. Therefore the number of admissible frequencies is limited, implying certain restrictions in frequency encoding. The presence of double-frequency, or envelope, oscillations makes it possible to extend frequency encoding, since the second frequency can play the role of a second encoding variable. Therefore, we can employ two coordinates for encoding instead of one.

In the paper by Borisyuk *et al.* (1992b) envelope oscillations are used to explain the experimental evidence recorded in the primary visual cortex (Gray and Singer, 1989; Gray *et al.*, 1990). Let us briefly discuss a preattention model which is based upon the idea that envelope oscillations play a significant role for the explanation of feature binding (Borisyuk *et al.*, 1994; Borisyuk and Borisyuk, 1995). During the information processing in the brain, a stimulus is presented as a set of separate features (for example, shape, color and so on) and each feature is presented by a spatio-temporal pattern of activity of a neural assemble. The basic principles and relative neural mechanisms are investigated to bind separate features and to create the whole image of the presented stimulus.

The preattention model is based of an idea of Damasio (Damasio, 1989) that feature binding occurs due to the coherence of neural activity in multiple regions of the neocortex which are linked together through activation of convergent zones. These zones, which are located in the higher levels of the neocortex, communicate through feedforward and feedback pathways to earlier zones of the primary cortex where different features of the stimulus are represented. In modeling low level information processing, we propose that feature binding should be sought in temporally coherent phase-locking of neural activity. This phase-locking is provided by one or more interacting convergent zones and does not require a central "top level" subcortical circuit (e.g. the septo-hippocampal system). Thus, this is an automatic, self-organizing synchronization of neural activity. To study feature binding in terms of synchronization of oscillations in a large scale system, we choose a Wilson–Cowan neural oscillator as the basic functional unit of the network. We consider a chain of locally coupled oscillators. Such a network can show different types of dynamic behavior: regular oscillations with various phase shifts, traveling waves, envelope oscillations, and chaotic oscillations (Bori-

syuk and Urzhumtseva, 1990; Borisyuk and Borisyuk, 1995). The morphological evidence and results presented there for two coupled (oscillators allow to control the chain and, by choosing parameters, to get the desirable dynamic behavior.

Thus, to model interactive convergent zones, we consider a two-layer neural network of two locally interacting chains of oscillators with excitatory to inhibitory connections inside each layer and local connections between excitatory subpopulations for interlayer communications. The chain of oscillators models an early neocortical zone responsible for the analysis of a single feature of a stimulus. The first layer of the network receives the external input signal (stimulus). The second layer corresponds to the upper convergent zone where the signals from the first layer are analysed.

Under stimulation by a simple stimulus (oscillators of some compact region receive high level of input signal and other ones receive zero signal) the oscillators of the first layer with high level of the input signal demonstrate synchronous envelope oscillations. The synchronization mode appears due to excitatory to inhibitory type of the local connections inside the layer and the envelope feature appears due to excitatory connections between layers. The synchronous activity is interpreted as the formation of an integral pattern related to the simple input stimulus.

When a complex stimulus (two compact non-overlapping regions of oscillators receiving the input signal of a high level, other oscillators receive zero input signal) is applied, however, the network responds by forming two corresponding non-overlapping areas of oscillatory activity in the first layer. This activity is represented by quasiperiodic (envelope) oscillations with two frequencies. The low frequency is about one-tenth of the high frequency. The high frequency oscillations are synchronous in each area, but there is no synchronization between the areas. However, the low frequency oscillations are synchronous for oscillators of both areas. Synchronization at a low frequency results from convergent connections between layers. The second layer provides envelope oscillations and is the source of low frequency synchronization. Thus, the synchronization of low frequency oscillations in

Figure 9. Low frequency synchronization using envelope oscillations. Complex stimulus is applied to two-layer neural network of two locally interacting chains of 13 oscillators with excitatory to inhibitory connections inside each layer and local connections between excitatory subpopulations for interlayer communications. (a) Complex stimulus profile with two areas of excitation A and B; (b) Three examples of dynamic behavior of different oscillators in the first layer: $E_4(t)$ and $E_5(t)$ belong to the excitated area A and $E_9(t)$ belongs to the excitated area B. Note characteristic envelope profile and synchronization between all shown oscillators at a low frequency. (c) Zoom of the previous picture showing that at a high frequency E_4 and E_5 work in-phase and they both work in anti-phase with E_9.

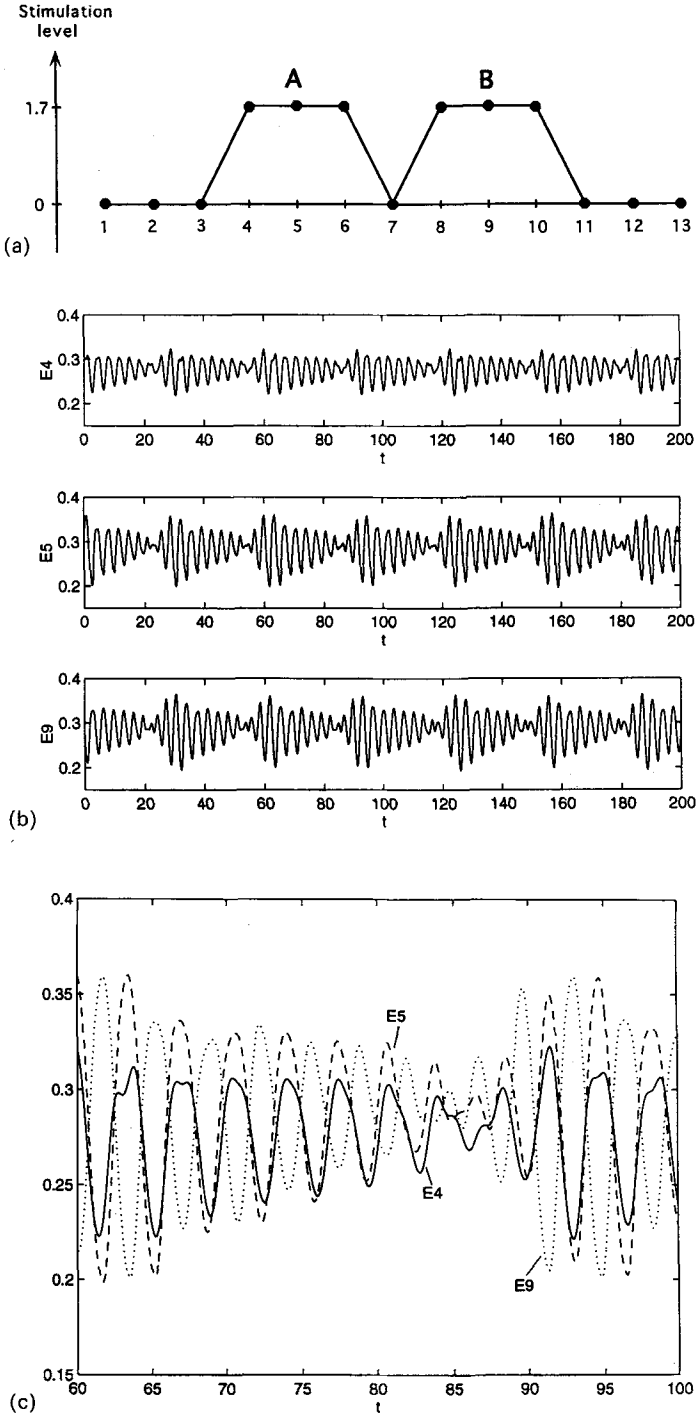

Figure 9. (a), (b) and (c).

different regions of the first layer arises due to the interactions between two convergent zones; it can be interpreted as a feature binding of a complex stimulus. Figure 9 shows the dynamics of the average activity ($E_i^1(t)$) of the excitatory neural subpopulations of the oscillators of the first layer under complex stimulus: $E_4^1(t)$ and $E_5^1(t)$ are taken from one stimulated area of the chain and $E_9^1(t)$ is taken from the other area. All these oscillations are envelope oscillations. One can see that E_4^1 and E_5^1 demonstrate synchronous oscillations (Fig. 9c). E_5^1 and E_9^1 demonstrate anti-phase high frequency oscillations (Fig. 9c) but low frequency components are synchronous (Fig. 9b).

R.M.B. is grateful to Prof. Wolf Singer for helpful discussions. A.I.K. appreciates careful reading of the paper and valuable comments from Prof. John Guckenheimer and Dr Mark Myers. The research of G.N.B. and R.M.B. was supported by the James S. McDonnell Foundation (Grant 93-9), International Science Foundation (Grant RMQ000) and Russian Foundation of Fundamental Research (Grant 94-01-01270a). The research of A.I.K. was supported by a Research Fellowship of the Katholieke Universiteit Leuven (Belgium) and by DOE. We would like to thank the referees for their useful comments.

APPENDIX. BIFURCATIONS OF LIMIT CYCLES IN A SYSTEM OF TWO COUPLED OSCILLATORS.

Consider bifurcations of limit cycles of symmetric (**SC**), antisymmetric (**AC**) and non-symmetric (**NC**) types that may occur in a model of two identical and symmetrically coupled two-dimensional oscillators with a varying parameter α, representing the strength of the coupling. We partially follow a paper which suggests a list of possible bifurcations (Nikolaev, 1995). However, the list is limited to local bifurcations.

For all values of α, a symmetric limit cycle **SC** lies in the two-dimensional plane L, invariant under the symmetry. Therefore, it may undergo two types of bifurcations: (1) bifurcations in the plane (planar bifurcations); and (2) bifurcations involving directions transversal to the plane. Depending on the type of coupling, planar bifurcations may be present or not in the system. They usually occur in the case of direct coupling as in model (2), but they never occur in the case of diffusion-type coupling.

A list of planar bifurcations includes: merging of **SC** with a symmetric equilibrium at an Andronov–Hopf bifurcation; the collision of **SC** with a distinct symmetric limit cycle at a fold bifurcation for limit cycles; and the disappearance of **SC** at a homoclinic orbit involving either a saddle or saddle-node in L, corresponding to a homoclinic bifurcation or a fold bifurcation, respectively.

Next, there are exactly two multipliers of **SC** that determine its stability in the normal directions to L. When one or both of them cross the unit circle bifurcations of the second kind occur. If one multiplier passes through the value $+1$, a symmetry-breaking bifurcation occurs, which leads to a pair of nonsymmetric limit cycles. Another possibility is that a multiplier passes through the value -1, which leads to a period doubling bifurcation and to the appearance of an antisymmetric limit cycle with (asymptotically) doubled period. Finally, both multipliers, forming a complex conjugate pair, may cross the unit circle. This corresponds to a torus, or Neimark–Sacker bifurcation, which leads to the appearance of an antisymmetric invariant 2-torus.

We now consider bifurcations of an antisymmetric limit cycle **AC**. Unlike **SC**, it is not planar, yet it is not generic, since it possesses some symmetry properties. **AC** cannot have just one multiplier at -1 and, therefore, it cannot undergo a period doubling bifurcation. However, other "generic" bifurcations are still possible. In particular, when a multiplier passes through $+1$ either a symmetry-breaking bifurcation occurs, leading to the appearance of a pair of nonsymmetric limit cycles, or a fold bifurcation for limit cycles, at which **AC** collides with another antisymmetric limit cycle so that they both disappear. To distinguish between these two cases, we should consider the so-called square root of the Poincaré mapping (cf. Nikolaev, 1995). If a pair of complex conjugate multipliers crosses the unit circle, a torus bifurcation occurs leading to the appearance of an antisymmetric torus. The limit cycle **AC** may disappear via merging with a symmetric limit cycle, when the latter undergoes a period-doubling bifurcation, and via merging with an equilibrium in L, when the latter undergoes an Andronov–Hopf bifurcation (with critical two-dimensional eigenspace transversal to L). Finally, **AC** may disappear at a homoclinic or heteroclinic bifurcation. Note that two homo- or heteroclinic orbits symmetric to each other should appear simultaneously. In the first case, they are both associated with a symmetric saddle equilibrium and together they form an antisymmetric figure-of-eight loop. In the second case, heteroclinic orbits are associated with two nonsymmetric saddles and together they form an antisymmetric heteroclinic contour.

A nonsymmetric limit cycle **NC** is a true generic limit cycle and therefore it may undergo any bifurcation allowed in generic systems. However, there are a few important remarks. The limit cycle **NC**, together with its image under the symmetry, may both merge with an antisymmetric limit cycle, or with a symmetric limit cycle, at a symmetry-breaking bifurcation. In both cases, a multiplier of **NC** approaches the value $+1$ when the critical parameter is approached. If **NC** stays far away from symmetric or antisymmetric invariant sets, then obviously bifurcations of **NC** generate only nonsymmetric invariant sets. For example, a torus bifurcation of **NC** give rise to a nonsymmetric 2-torus. Clearly, nonsymmetric limit cycles forming a symmetric pair bifurcate simultaneously and in the same fashion.

The bifurcations mentioned above can occur in several ways. This is reflected in the following terminology. A bifurcation is called *forward* or *backward* if, when a critical parameter value is passed, the bifurcating object becomes less or more stable, respectively. This terminology reflects the direction of the parameter change near the critical point, in invariant terms. A bifurcation is called *supercritical* if a new invariant set emanates from the bifurcating one in those parameter direction where the latter set shows less stability, and *subcritical* if it emanates in the reverse direction. Usually, a bifurcation is assumed forward and supercritical, by default.

REFERENCES

Abbott, L. F. 1990. A network of oscillators. *J. Phys. A: Math. & Gen.* **23,** 3835–3859.

Arnold, V. I. 1983. *Geometric Methods in the Theory of Ordinary Differential Equations*. Berlin: Springer-Verlag.

Aronson, D., G. B. Ermentrout and N. Kopell. 1990. Amplitude response of coupled oscillators. *Physica D* **41,** 403–449.

Baird, B. 1986. Nonlinear dynamics of pattern formation and pattern recognition in the rabbit olfactory bulb. *Physica D* **22,** 150–175.

Borisyuk, R. M. 1991. Interacting neural oscillators can imitate selective attention. In *Neurocomputers and Attention. Neurobiology, Synchronization and Chaos*, A. V. Holden and V. I. Kryukov (Eds), pp. 189–200. Manchester: Manchester University Press.

Borisyuk, R. M. and L. M. Urzhumtseva. 1990. Dynamical regimes in a system of interacting neural oscillators. In *Neural Networks—Theory and Architecture*, A. V. Holden and V. I. Kryukov (Eds), pp. 9–20. Manchester: Manchester University Press.

Borisyuk, R. M. and A. B. Kirillov. 1992. Bifurcation analysis of a neural network model. *Biol. Cybern.* **66,** 319–325.

Borisyuk, R. and G. Borisyuk. 1995. Complex dynamic behavior of oscillatory neural networks: examples and application. *Proc. of WCNN'95* (submitted).

Borisyuk, G. N., R. M. Borisyuk, A. B. Kirillov, V. I. Kryukov and W. Singer. 1990. Modelling of oscillatory activity of neuron assemblies of the visual cortex. In *Proc. of Intern. Joint Conf. on Neural Networks—90*, **2,** San-Diego, 431–434.

Borisyuk, G. N., R. M. Borisyuk, Ya. B. Kazanovich, T. B. Luzyanina, T. S. Turova and G. S. Cymbalyuk. 1992a. Oscillatory neural networks. Mathematics and applications. *Math. Modeling* **4,** 3–43 (in Russian).

Borisyuk, G. N., R. M. Borisyuk and A. I. Khibnik. 1992b. Analysis of oscillatory regimes of a coupled neural oscillator system with application to visual cortex modeling. In *Neural Network Dynamics*, J. G. Taylor, E. R. Caianiello, R. M. J. Coterill and J. W. Clark (Eds). Springer Series Perspectives in Neural Computing, pp. 208–226. Berlin: Springer-Verlag.

Borisyuk, G., R. Borisyuk, Y. Kazanovich and G. Strong. 1994. Modeling the binding problem and attention by synchronization of neural activity. In *SPRANN'94 IMACS International Symposium on Signal Processing, Robotics and Neural Networks*, Lille, France.

Cymbalyuk, G. S., E. V. Nikolaev and R. M. Borisyuk. 1994. In-phase and antiphase self-oscillations in a model of two electrically coupled pacemakers. *Biol. Cybern.* **71,** 153–160.

Damasio, A. R. 1989. The brain binds entities and events by multiregional activation from converges zones. *Neural Comput.* **1,** 123–132.

Dmitriev, A. S. 1993. Chaos and information processing in nonlinear dynamical systems. *Radiophys. Electronics* **38,** 1–24 (in Russian).

Eckhorn, R., R. Bauer, W. Jordan, M. Brosch, W. Kruse, M. Muk and H. J. Reitboeck. 1988. Coherent oscillations: a mechanism of feature linking in the visual cortex? *Biol. Cybern.* **60,** 121–130.

Ermentrout, G. B. and J. D. Cowan. 1979. Temporal oscillations in neuronal nets. *J. Math. Biol.* **7,** 265–280.

Ermentrout, G. B. and N. Kopell. 1991. Multiple pulse interactions and averaging in systems of coupled neural oscillators. *J. Math. Biol.* **29,** 195–217.

Fenichel, N. 1971. Persistence and smoothness of invariant manifolds for flows. *Indiana Univ. Math. J.* **21,** 193–226.

Finkel, L. H. and G. M. Edelman. 1989. Integration of distributed cortical systems by reentry: A computer simulation of interactive functionally segregated visual areas. *J. Neurosci.* **9,** 3188–3208.

Freeman, W. J., 1987. Simulation of chaotic EEG patterns with a dynamical model of the olfactory system. *Biol. Cybern.* **56,** 139–150.

Freeman, W. J. 1991. The physiology of perception. *Scient. American* **2,** 34–41.

Freeman, W. J., Y. Yao and B. Burke. 1988. Central pattern generating and recording in olfactory bulb: a correlation learning rule. *Neural Networks* **1,** 277–288.

Gambaudo, J., P. Glendinning and C. Tresser. 1988. The gluing bifurcation I: symbolic dynamics of the closed curves. *Nonlinearity* **1,** 203–214.

Gray, C. M., P. König, A. K. Engel and W. Singer. 1989. Oscillatory responses in cat visual cortex exhibit inter-columnar synchronization which reflects global stimulus properties. *Nature* **338,** 334–337.

Gray, C. M., P. König, A. K. Engel and W. Singer. 1990. Synchronization of oscillatory responses in visual cortex: a plausible mechanism for scene segmentation. In *Synergetics of Cognition*. H. Haken and M. Stadler (Eds). Springer Series in Synergetics **45,** pp. 82–98. Berlin: Springer-Verlag.

Gray, C. M. and W. Singer. 1989. Stimulus-specific neuronal oscillations in orientation columns of cat visual cortex. *Proc. Natl. Acad. Sci. USA* **86,** 1698–1702.

Guckenheimer, J. and Ph. Holmes. 1983. *Nonlinear Oscillations, Dynamical Systems, and Bifurcations of Vector Fields*. Berlin: Springer-Verlag.

Hansel, D., G. Mato and C. Meunier. 1993. Phase dynamics for weakly coupled Hodgkin–Huxley neurons. *Europhys. Lett.* **23,** 367–372.

Hindmarsh, J. L. and R. M. Rose. 1982. A model of the nerve impulse using two first-order differental equations. *Nature* **296,** 162–164.

Kawato, M., M. Sokabe and R. Suzuki. 1979. Synergism and antagonism of neurons caused by an electrical synapse. *Biol. Cybern.* **34,** 81–89.

Kazanovich, Y. B., V. I. Kryukov and T. B. Luzyanina. 1991. Synchronization via phase-locking in oscillatory models of neural networks. In *Neurocomputers and Attention. Neurobiology, Synchronization and Chaos*, A. V. Holden and V. I. Kryukov (Eds), pp. 269–284. Manchester: Manchester University Press.

Kelso, J. A. S., J. P. Scholz and G. Schöner. 1986. Nonequilibrium phase transitions in coordinated biological motion: critical fluctuations. *Phys. Lett. A* **118,** 279–284.

Khibnik, A. I. 1990. *Using TraX: A Tutorial to Accompany TraX, A Program for Simulation and Analysis of Dynamical Systems*. Setauket, New York: Exeter Software.

Khibnik, A. I., R. M. Borisyuk and D. Roose. 1992. Numerical bifurcation analysis of a model of coupled neural oscillators. In *Bifurcation and Symmetry: Cross Influences between Mathematics and Applications*, E. L. Allgower, K. Boehmer and M. Golubitsky (Eds), Int. Ser. Numer. Math. **104,** pp. 215–228. Basel: Birkhauser.

Khibnik, A. I., Yu. A. Kuznetsov, V. V. Levitin and E. V. Nikolaev. 1993a. Continuation techniques and interactive software for bifurcation analysis of ODEs and iterated maps. *Physica D* **62,** 360–371.

Khibnik, A. I., Yu. A. Kuznetsov, V. V. Levitin and E. V. Nikolaev. 1993b. *LOCBIF: Interactive LOCal BIFurcation Analyser (version* 2). Amsterdam: Computer Algebra Netherlands Expertise Center.

König, P. and T. B. Schillen. 1991. Stimulus dependent assembly formation of oscillatory responses: I. Synchronization. *Neural Comput.* **3,** 155–166.

Kopell, N. 1988. Toward a theory of modeling central pattern generators. In *Neural Control of Rhythmic Movements in Vertebrates*, A. H. Cohen, S. Rossignol and S. Grillner (Eds), pp. 369–413. New York: Wiley.

Kryukov, V. I. 1991. An attention model based on the principle of dominanta. In *Neurocomputers and Attention. Neurobiology, Synchronization and Chaos*, A. V. Holden and V. I. Kryukov (Eds), pp. 319–352. Manchester: Manchester University Press.

Kryukov, V. I., G. N. Borisyuk, R. M. Borisyuk, A. B. Kirillov and E. L. Kovalenko. 1990. Metastable and unstable states in the brain. In *Stochastic Cellular Systems: Ergodicity, Memory, Morphogenesis*, R. L. Dobrushin, V. I. Kryukov and A. L. Toom (Eds), pp. 225–357. Manchester: Manchester University Press.

Levitin, V. V. 1989. *TraX: Simulation and Analysis of Dynamical Systems*. Setauket, New York: Exeter Software.

Li, Z. and J. J. Hopfield. 1989. Modeling the olfactory bulb and its oscillatory processing. *Biol Cybern.* **61,** 379–392.

MacGregor, R. J. 1987. *Neural and Brain Modelling*. New York: Academic Press.

Malkin, I. G. 1956. *Some Problems of the Theory of Nonlinear Oscillations*. Moscow: Gostehizdat (in Russian).

Malsburg, von der, C. and W. Schneider. 1986. A neural cocktail-party processor. *Biol Cybern.* **54,** 29–40.

Miller, R. 1991. *Cortico-Hippocampal Interplay*. Berlin: Springer-Verlag.

Nicolis, J. S. 1990. *Chaos and Information Processing. A Heuristic Outline*. Singapore: World Scientific.

Nicolis, J. S. and I. Tsuda. 1985. Chaotic dynamics of information processing—the "magic number seven plus-minus two" revised. *Bull. Math. Biol.* **47,** 343–365.

Nikolaev, E. V. 1995. Bifurcations of limit cycles of differential equations invariant under involutory symmetry. *Matemat. Sbornik.* **186,** 143–160 (in Russian).

Schillen, T. B. and P. König. 1991. Stimulus dependent assembly formation of oscillatory responses: II. Desynchronization. *Neural Comput.* **3,** 167–177.

Schöner, G., W. Y. Jiang and J. A. S. Kelso. 1990. A synergetic theory of quadrupedal gaits and gait transitions. *J. Theor. Biol.* **142,** 359–391.

Schutter, E. De, T. W. Simon, J. D. Angstadt and R. L. Calabrese. 1993. Modeling a neural oscillator that paces heartbeat in the medicinal leech. *Amer. Zool.* **33,** 16–28.

Shinomoto, S. 1987. A cognitive and associative memory. *Biol Cybern.* **57,** 197–206.

Shuster, H. G. and P. Wagner. 1990a. A model for neuronal oscillations in the visual cortex. I: Mean-field theory and derivation of phase equations. *Biol. Cybern.* **64,** 77–82.

Shuster, H. G. and P. Wagner. 1990b. A model for neuronal oscillations in the visual cortex. II: Phase description of feature dependent synchronization. *Biol Cybern.* **64,** 83.

Skeldon, A. C. 1994. Dynamics of parametrically excited double pendulum. *Physica D* **75,** 541–558.

Sompolinsky, H., D. Golomb and D. Kleinfild. 1990a. Global processing of visual stimuli in a neural network of coupled oscillators. *Proc. Natl. Acad. Sci. USA* **87,** 7200–7204.

Sompolinsky, H., D. Golomb and D. Kleinfild. 1990b. Phase coherence and computation in neural network of coupled oscillators. In *Non-linear Dynamics and Neuronal Networks*, W. Singer and H. G. Schuster (Eds). Weinheim: VCW Verlag.

Sompolinsky, H., D. Golomb and D. Kleinfild. 1991. Cooperative dynamics in visual processing. *Phys. Rev. A* **43,** 6990–7011.

Sporns, O., J. A. Gally, G. N. Reeke and G. M. Edelman. 1989. Reentrant signaling among simulated neuronal groups leads to coherency in their oscillatory activity. *Proc. Natl. Acad. Sci. USA* **86,** 7265–7269.

Tsuda, I. 1992. Dynamic link of memory—chaotic memory map in nonequlibrium neural networks. *Neural Networks* **5,** 313–326.

Vinogradova, O. S., E. S. Brazhnik, V. S. Stafekhina and A. B. Belousov. 1991. Septo-hippocampal system. Rhythmic oscillations and information selection. In *Neurocomputers and Attention. Neurobiology, Synchronization and Chaos*, A. V. Holden and V. I. Kryukov (Eds), pp. 129–148. Manchester: Manchester University Press.

Wang, D. L., J. Buhmann and C. von der Malsburg. 1990. Pattern segmentation in associative memory. *Neural Comput.* **2,** 94–106.

Wang, X.-J. and J. Rinzel. 1992. Alternating and synchronous rhythms in reciprocally inhibitory model neurons. *Neural Comput.* **4,** 84–97.

Wang, X.-J. and J. Rinzel. 1993. Spindle rhythmicity in the reticularis thalami nucleus: sinchronization among mutually inhibitory neurons. *Neurosci.* **53,** 899–904.

Wilson, M. A. and J. M. Bower, 1988. A computer simulation of olfactory cortex with functional implications for storage and retrieval of olfactory information. In *Neural Inform. Proc. Syst.*, D. Anderson (Ed.), pp. 114–126. New York: AIP Press.

Wilson, H. R. and J. D. Cowan. 1972. Excitatory and inhibitory interactions in localized populations of model neurons. *Biophys. J.* **12,** 1–24.

Yao, Y. and W. J. Freeman. 1990. Model of biological pattern recognition with spatially chaotic dynamics. *Neural Networks* **3,** 153–170.

Yao, Y., W. J. Freeman, B. Burke and Q. Yang. 1991. Pattern recognition by a distributed neural network: an industrial application. *Neural Networks* **3,** 153–170.

Received 3 January 1993
Revised version accepted 7 March 1995